

VORTICAL FLOW PATTERNS FOR HIGH LIFT FOR HIGH SPEED AIRCRAFT CONCEPTS

J-E. Lombard^{*****}, P. Leyland^{*}, M. Gaffuri ^{**}, Y. Wohlhauser ^{***}

Interdisciplinary Aerodynamics Group, GR-SCI-IAG, EPFL, Station 9, 1015 Lausanne, Switzerland, email:penelope.leyland@epfl.ch; ** DLR-Braunschweig, Germany; **presently PhD student, Imperial College London, UK; ***Bosch Research, Solothurn, Switzerland*

Abstract

Enhancing detached vortical flow over leading edges and flap surfaces allow high lift configurations in critical regimes of take-off and acceleration. In the context of the FP6 Environmentally Friendly High Speed Aircraft project HISAC, future high speed aircraft concepts were studied. Specific morphed leading edges were devised that are adapted to ultra-fine wing geometries, and enhance lift. Unsteady CFD and Wind Tunnel tests for low speed were based on the FP6 EPISTLE project (European Project for the Improvement of Supersonic Transport Low Speed Efficiency). Similar situations arise for high speed fighter aircraft at low speeds, where integrated flap design is optimised for assuring high lifting vorticity over the leeward side. Again CFD and wind tunnel testing were performed producing qualitative agreement.

1. Introduction

One of the critical parts of the design of novel concepts of environmentally friendly and efficient high speed aircraft for the future are leading edge devices for the low speed off-design regimes such as near take-off, high angle of attack situations for highly swept wings, where high –lift enhancement is required. In the context of two European projects under the 6th framework programme (FP6), EPISTLE and HISAC, [1],[2], conducted respectively under the responsibility of Airbus and Dassault Aviation, high level simulations (CFD) were performed to evaluate and validate the prediction of low speed flows on a supersonic aircraft wing featuring specific design high-lift devices and compared to wind tunnel tests.

One of the design challenges for high speed aircraft including supersonic cruise regimes is that the extremely slender low aspect ratio swept wings, especially at their leading edges (LE), limit the space for housing servo-mechanical systems for LE flap deployment and retraction. The EPISTLE wing concepts produced a generic concept with morphing blunted leading edges that maintain the vortices on the suction side of the leading edge, [3].

The capability of CFD tools to predict the low-speed flows over high-lift systems, especially at off-design conditions such as high angles of attack remains a challenging task. The vortex enhanced lift and the vortex formations emanating from zones on or near to the leading edge shapes for such high swept wings promotes such challenges for state of the art CFD and associated turbulence modelling.

Wind tunnel data are available from the EPISTLE project from testing in the ONERA-F1 wind tunnel of such a supersonic wing model with specific morphed leading edges, scaled to 1:22. The model is provided with a fixed main wing structure and trailing edge flaps. Three interchangeable leading edges (LE) are manufactured representing different high lift system configurations. The geometry considered here is the so called deep hinge configuration. The wing was mounted on a three-strut balance and extensively equipped with pressure taps located on the main wing and the morphed LE slat.

Another high speed aircraft design configuration concerning vortex optimisation is the use of leading edge extension (LEX) flaps at subsonic speeds which divert the vortices away from the vertical tail plane, moving the maximum suction region towards the wing tips while partially re-attaching the flow during high angle of attack situations and manoeuvres. Such structures are notably interesting for aircraft configurations with engine integration between the fuselage and the wing's LE, as for fighters. Indeed, large-scale unsteady vortices are shed from the forebody, the leading edges, LEX flaps and strakes creating important lift effects, although their unsteadiness could render manoeuvring difficulties and fatigue. A low speed wind tunnel and water tunnel experimental campaign was performed by ETHZ, on such an aircraft configuration, [4].

In this paper the prediction of such complex flows with vortical structures is investigated using Computational Fluid Dynamics (CFD), tuning the highly sensitive parameters of numerical schemes, turbulence modelling, and grid resolution. Steady state and time-accurate combined with second and fourth order spatial accurate numerical schemes Reynolds-averaged Navier-Stokes (RANS) computations are performed and compared to the experimental data. The use of high level visualisation software for computing the vortex core path and rendering the iso-pressure and iso-vorticity surfaces as well as streamlines and surface skin-friction, provides an important analysis tool,[5].

Comparisons of several codes for the EPISTLE geometry are made in the paper [13], presented at the AIAA conference 2013 at the same time as this EUCASS conference, based on a recent DLR-JAXA collaboration on supersonic flow. The work presented here was performed by the authors for the HISAC project and were compared favourably to other partners.

The paper is organised as follows: firstly the geometry and computational meshes are described for the EPISTLE model and then for a model of a LEX flap based on a simplified wind-tunnel forebody geometry of the Sukhoi PAK-FA that uses a movable LEX. Then the computational methods are discussed, and the results given. Finally some conclusions and future perspectives are given

2. Geometries and computational meshes

2.1 The EPISTLE geometry and mesh generation

The EPISTLE model was a 1:22 scaled model of a next generation supersonic transport aircraft. The model was approximately of size 4mX2m with a chord of about 1.2 m and was mounted on a three-strut balance inside the ONERA-F1 wind tunnel measurement chamber. The model is provided with a fixed main wing structure and trailing edge flaps. Three interchangeable leading edges (LE) are manufactured representing different high lift system configurations. The geometry considered here is the so-called deep hinge configuration. The main flow condition was taken to be $AoA=11.22^\circ$; $Mach=0.25$; $Re=22.5 \times 10^6$, and the complete polar was generated from -2 to +20 AoA.



Figure 1: The EPISTLE model placed with the ONERA F1 wind tunnel

The meshes were generated with ANSYS ICEMCFD. Unstructured hybrid meshes of layers of prisms (boundary layer), pyramids (mesh transition) and tetrahedra, and block-structured hexahedral meshes were generated.

The unstructured mesh was of approximately 4 million cells and formed a hemispherical domain around the EPISTLE geometry. This allowed an initial obtain a first impression of the flow and the use of an unstructured solver for comparison. As the first cell height is at about $y^+=50$, the technique of wall functions

has to be activated to correctly in the RANS simulations. The mesh is refined where the physical gradients are high and where the curvature of the geometry is important (Fig. 2). In this mesh, the cells in the wake are unfortunately rather coarse, since the volume mesh was generated using a constant ratio for the cells' radial growth around the airplane.

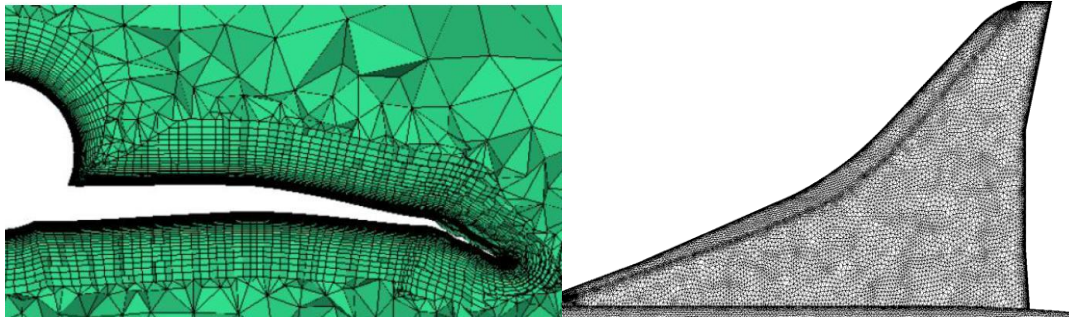


Figure 2: EPISTLE wing LE: 4 million cell prismatic/tetra unstructured mesh (left) and view over the wing span for a coarsened version (1.8 million) right.

The multiblock structured mesh was generated with ICENCFD HEXA, and was composed of 12.6 million hexahedral cells that are disposed in C grid layers around the wing and the fuselage of the airplane (topo B). The height of the first layer is at $y^+ < 1$ allowing calculations without wall functions. Very fine thin blocks were built along the leading edge and the wing tip. This allows a better control of the mesh parameters at this strategic location and avoids a compression of the cells between the slat and the wing tip. An initial topology blending C grids and body fitted O grids was also generated, however the quality was less conclusive, (topo A).

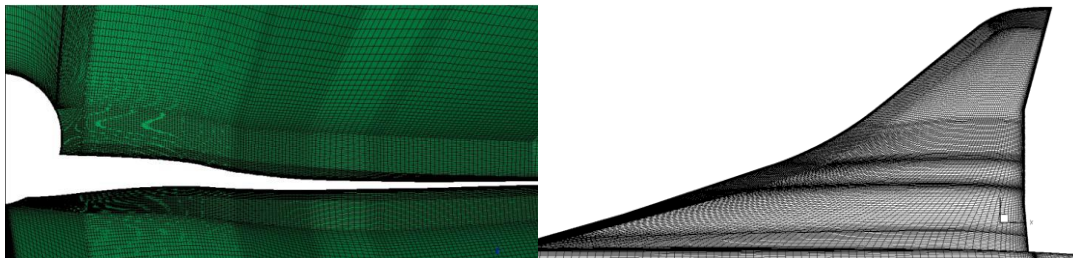


Figure 2: EPISTLE wing LE: 12.6million hexahedral cell, lateral cut (left) and view over the wing span (right).

All computational meshes were checked for quality using ICEMCFD in-built quality histograms, and running basic calculations to scan for values of y^+ , detect zones insufficiently refined, and improve the blocking strategies. Coarser meshes were generated and run for initial parameter fixes.

2.2 The LEX geometry and mesh generation

A CAD model of a simplified PAK-FA was rebuilt from a model airplane and a water tunnel. A 5% scale flat plate wing-body model approximation to the complex delta-wing is used with sharp leading edges, with a 3D fore-body. The model has a 73.5cm wing span, 25 cm² reference wing area, a mean aerodynamic chord (MAC) of 4:355cm, with an aspect ratio of 2.16. The wind tunnel was the subsonic tunnel at ETHZ with fans that can provide 2250[Pa] of dynamic pressure and wind velocity scales linearly with the power of the fans [6]. The velocity profile can be considered homogeneous away from the walls. At 18[m/s] turbulent intensity is measured to be 0.62%. The computational grids were again generated with ICEMCFD HEXA, and the computational domain was taken to be the exact wind tunnel dimensions. The final grid was of the order of 32 million cells of 2064 blocks, and a non-

conformal interface was placed between the LEX flap and the flat plate. A $y^+ < 1$ was achieved over the entire body of the aircraft model and the wind-tunnel wall. Two angles of LEX deflection are considered at 0 and 20°.

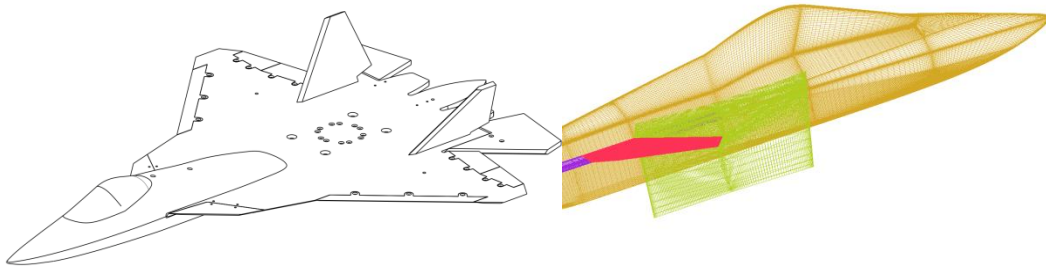


Figure 3: Generic PAK-FA simplified by a flat plate extension (left); LEX Flap shown in red, surface mesh and non-conformal plane shown in green to assure mesh blocking between the fuselage and the different deflecting angle LEX flap (right).

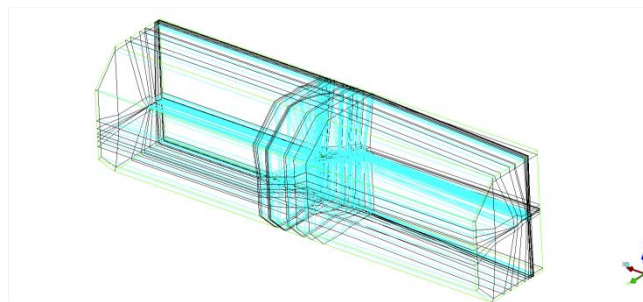


Figure 4: Computational domain for the LEX geometry: reproducing exactly the wind tunnel geometry shape.

3. Results

3.1 Computational Codes

For the EPISTLE geometry, two codes were used, the NSMB code or the Metacomp Technologies CFD++ code. For the LEX geometry only the NSMB solver was employed. The calculations were performed using the parallel MPI versions, either on the Cray XT3 cluster at CSCS for EPISTLE or on the local Linux cluster pleiades2 at EPFL for both EPISTLE and LEX. Visualisations of the results were made using the BASPL++ software from SMR Engineering that contains time-accurate algorithms for vortex core tracking, [7][5].

CFD++ is a Computational Fluid Dynamics (CFD) software package designed by Metacomp Technologies, Inc., to tackle a wide range of problems encountered in aerospace, automotive, biomedical and other areas. The CFD++ software suite can handle unstructured meshes of hybrid type and structured meshes.

NSMB works on block-structured hexahedral meshes that can be patched. NSMB is a code originally developed at EPFL and then extended to the NSMB consortium, which included several universities (EPFL, ETHZ, SERAM, IMF-Toulouse, IMF-Strasbourg, KTH, TUM), research establishments (CERFACS), and industrial partners EADS-France (Airbus France and EADS Space Technologies), and CFS Engineering, [8][9].

The space discretisation schemes implemented in NSMB include:

- 2nd-order and 4th-order Central scheme with artificial dissipation (standard Jameson scheme dissipation, Martinelli dissipation or matrix dissipation)
- Upwind schemes (Roe, AUSM+, HLLE, Riemann scheme), 2nd and 3rd order using the MUSCL approach with various limiters, 5th order using Weighted ENO

The steady state calculations can be made using either the explicit Runge Kutta scheme or the implicit LU-SGS scheme. Convergence acceleration methods include: Local time stepping, Full multi-grid (grid sequencing), Pre-conditioning for low Mach number flows.

Several turbulence models are implemented and well tested including, Spalart-Allmaras 1 equation turbulence model (low and high speed models), Chien $k-\epsilon$ 2-equation model, Wilcox $k-\omega$ 2-equation turbulence model and the Baseline and Shear stress $k-\omega$ 2-equation turbulence models of Menter. [10-12]
NSMB includes also several Large Eddy Simulation models.

3.2 Results Epistle

The CFD assessment on the EPISTLE model with long hinge configuration were considered for the aerodynamic free stream conditions

- o Angle of attack: $\alpha=11.22^\circ$ (with wind-tunnel corrections)
- o Mach: $M=0.25$
- o Reynolds Number: $Re= 22.4584 \times 10^6$
- o Stagnation Pressure: 338,156 Pa
- o Stagnation Temperature: 301.1 K
- o Static Pressure: $P=323,613$ Pa
- o Temperature: $T=297.3$ K.

In order to enhance the CFD assessment, a Polar ranging between 5° and 20° AoA with fine discretisation around the maximum L/D was available.

When using CFD++ on the unstructured mesh, the RANS mode was chose using a preconditioning based on a fraction of maximum velocity. Turbulence modelling was taken to be the cubic k -epsilon model, which is based on the average turbulent kinetic energy and the average turbulence dissipation rate.

The time integration was chosen implicit, the courant number was ramped between 1 and 250, and the calculation was stopped automatically, if the residuals would have come below 10^{-8} . Spatial discretisation was of second order and the calculation ran with double precision.

For NSMB, LU-SGS implicit time stepping was taken for steady state calculations, and embedded in dual – time stepping for transient calculations. The spatial discretisation was taken to be either the second order central scheme with fourth order artificial dissipation or the 4th order central scheme seems to be the most adapted settings to match the experimentation, at least at 11.22° AoA, and can be used as reference simulation for comparisons with other partners of the HISAC WP2 Task 2.5 project. Both the Mentor's $k-\omega$ SST and the Spalart Almaras turbulent models were used. Approximately 5 double dual core processors were used for symmetric viscous simulations for the 12.6 millions cell mesh for calculation times upto 30 hours, depending on the simulation type and the chosen turbulence model.

In Table 1 it can be seen that the aerodynamic values are similar for the different solvers and degrees of refinement of the mesh. However, further analysis shows that only the 12 million structured mesh elements were sufficient to reproduce the L/D polar with an accuracy better than 1% relative to the experimental results.

Solution at 11.22 deg angle of attack			
	CD	CL	Cm
Wind Tunnel Test	0.041	0.423	0.087
<i>Unstructured mesh</i>			
CFD++	0.046	0.412	-
<i>Structured mesh</i>			
Topo. A - NSMB 2 nd order	0.052	0.420	0.086
Topo. B - NSMB 2 nd order	0.045	0.438	0.096
Topo. B - NSMB 4 th order	0.044	0.432	0.092

Table 1: Aerodynamic coefficients different solvers: Values are multiplied by a scale factor.

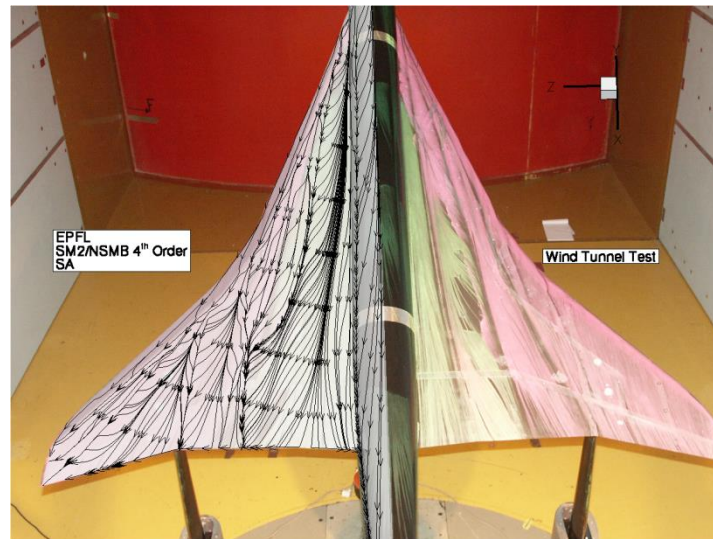


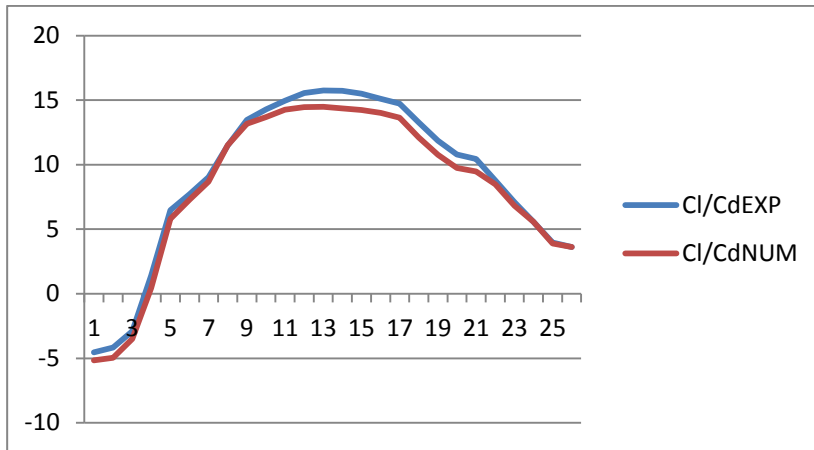
Figure 5: Comparison Wind Tunnel EPISTLE Skin friction lines at $AoA=11.22^\circ$; $Mach=0.25$; $Re=22.5 \times 10^6$ with NSMB 4th-order; Spalart Almaras turbulence model (Courtesy HISAC WP2 Co-ordinator)

Comparison between wind tunnel skin friction lines and those computed from CFD show a good qualitative agreement. The vortices generated at wing root and wing crank are made in evidence in experiment and are numerically indicated. However, the polars are the most important values with the comparisons of the aerodynamic forces and coefficients. These show excellent agreement which implies that confidence can be made in the impressive vorticity representations given in the following figures.

The influence of the order of the flow solver is analysed on the structured mesh “SM2” (with topology “B”). For this purpose, the code EPFL-NSMB ran twice, once with the second-order central scheme and then with the fourth-order. The resulting aerodynamic coefficients and the deviation from the experimental data are presented respectively. As expected, the use of high order numerical scheme improves the accuracy of the flow solution and decreased the deviation from experiment by 50% the lift and pitching moment and by 20% the drag. The influence of the order of the flow solver is analysed in Table 2, the code NSMB is run with the second-order central scheme and the fourth-order one. The resulting aerodynamic coefficients and the deviation from the experimental data are presented. As expected, the use of high order numerical scheme improves the accuracy of the flow solution and decreased the deviation from experiment by 50% the lift and pitching moment and by 20% the drag. In particular, we are able to predict the behaviour of the lift to drag ratio for a large range of lift. The deviation from experiment remains within ± 1 (blue lines) except near the maximum L/D that is underestimated by 1.25 (8%) (see Table 3).

EPISTLE Aerodynamic coefficients at 11.22 deg. angle of attack						
Solution	ΔCL		ΔCD		ΔCm	
EPFL;SM2/NSMB 2 nd -order;SA	1.4 lc	3.4 %	48 dc	12.2 %	0.0085	10.1%
EPFL;SM2/NSMB 4 th -order;SA	0.8 lc	1.9 %	38 dc	9.7 %	0.005	5.5%

Table 2: Influence of the order of the scheme on the numerical aerodynamic coefficients at $AoA=11.22^\circ$; $Mach=0.25$; $Re=22.5 \times 10^6$. Deviation from the experimental data in absolute value and in percentage of the aerodynamic coefficients according to the order of the scheme (lc=lift count; dc=drag count).



Maximum lift to drag ratio			
Solution	Max L/D	Deviation from experiment	AoA
WTT	15.76	—	6.56
EPFL;SM2/NSMB 2 nd -order;SA	14.48	-8%	6.56

Table 3: Maximum lift to drag ratio experimentally measured and numerically predicted.

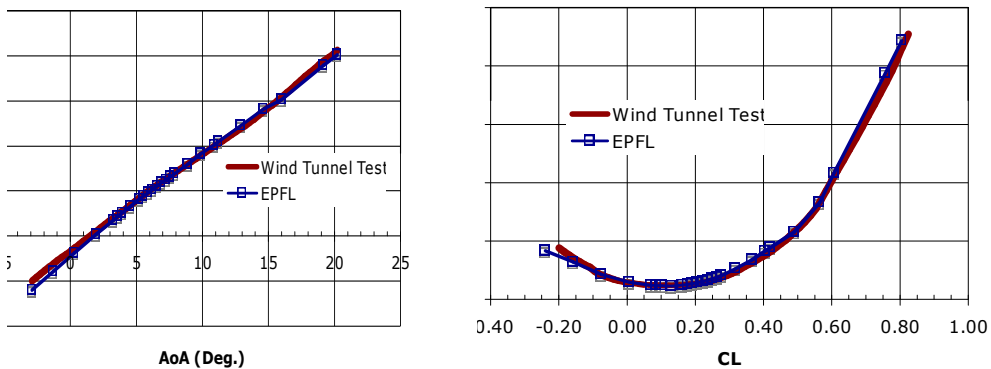


Figure 6: Lift Polar (left) and CD/CL Polar (right)

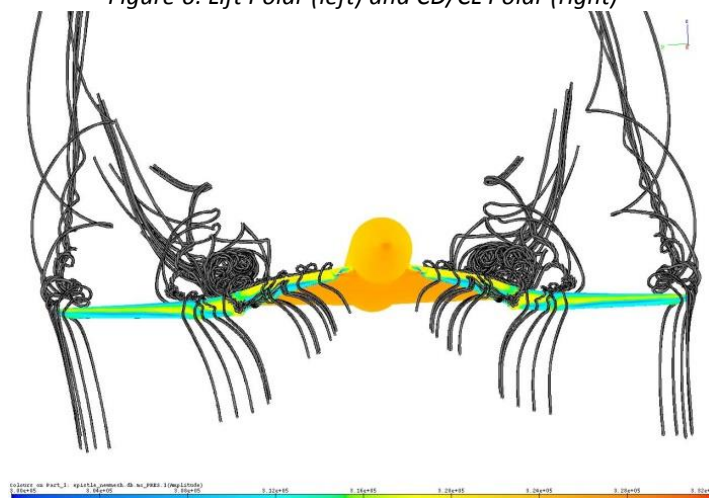
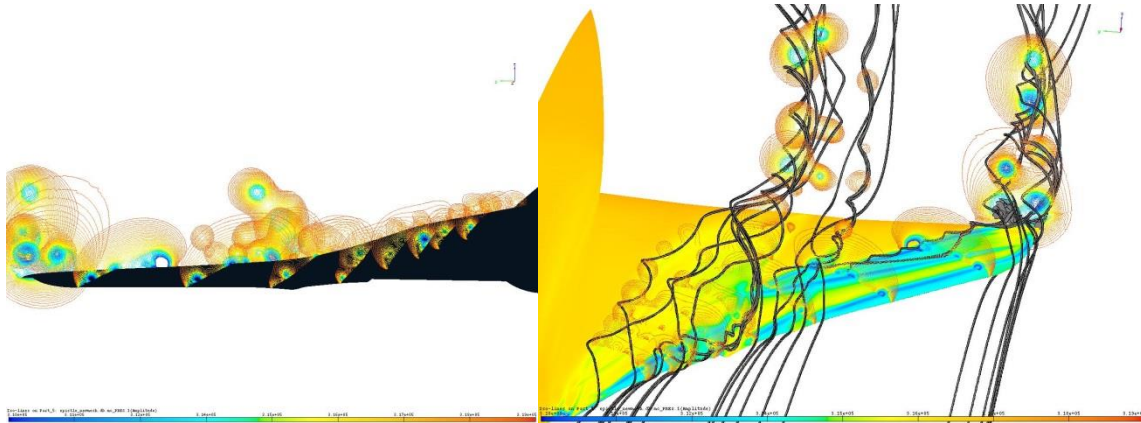
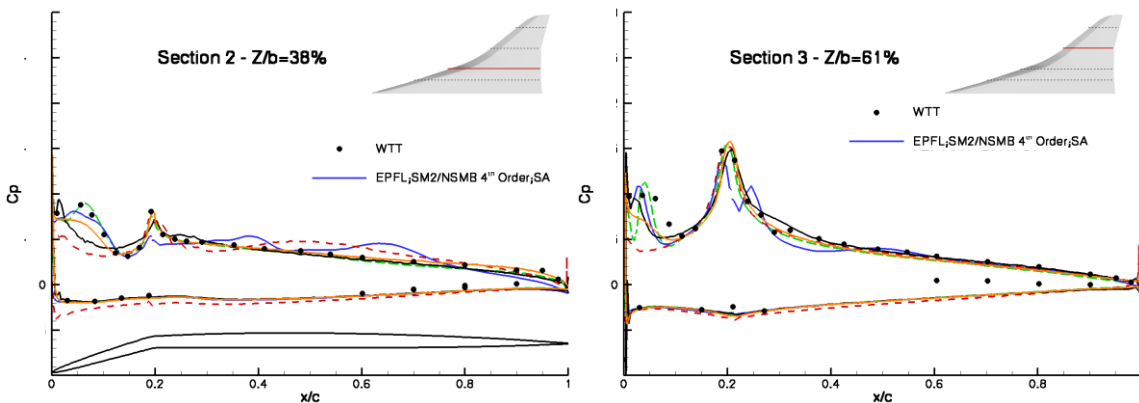


Figure 7: Vortex core evolution: tracking the vortex evolution from near the LE (view from front). The surface of the model is coloured by pressure levels.



Figures 8: EPISTLE: Vortex evolution with the vortex cores in cut planes along the wing, coloured by the total pressure levels (left). On the right, iso-pressure surfaces are given on the wing, and again the vortex cores coloured according to total pressure are superposed onto the streamlines.



Figures 9: EPISTLE: Pressure levels compared to experimental data along a specific cut along the spanwise direction. The position of the cut is show by the red line on the wing and correspond to 38% of the spanwise extent (left) and 61% (right). EPFL's results are given by the blue curve.

The vortices product a suction effect that enables a lift enhancement, their precise quantification is hence extremely important for off-design conditions. Their estimation has been noted to be influenced by the choice of the turbulence model, [13]. The relative size of vortices on the different leading edge parts defines the extent of positive pressure gradient upstream of the morphed flap's hinge line.

In Figures 7 and 8, the vortex core patterns are illustrated. in Figure 7 the general view of the vortices emanating from distinct LE or near LE locations over the wing are shown, whereas in Figure 8 details of the vortices and their cores are given along different sections, coloured according to isolines of total pressure. (where the vortex cores appear as circular locations of lower pressure). Iso-pressure levels are indicated on the wing surface. These views of cutting planes with pressure isolines combined with streamlines and p-isolines show five dominant separation vortices on the suction side of the wing, that came together to form a total of six vortices in the wake of the airplane, as well as smaller "satellite vortices" that are rotating around the main vortices. This was also confirmed by the pressure levels on the wing compared to the measurements, Figure 9.

The use of an accurate vortex core tracking algorithm in the visualisation software tool, BASPL++, allows the rendering of these important aspects, showing the positioning of the main vortexes with respect to the morphed integrated flap and hinges of the LE, the evolution of vorticity and the impact on the pressure levels on the suction side. [7][5].

Within this first part, the work concentrated on flow prediction around the EPISTLE candidate of a SCT-Supersonic Commercial Transport - featuring delta wing and morphed high-lift devices. The prediction capability is assessed at $AoA=11.22^\circ$, $Mach=0.25$ and $Re=22.5 \times 10^6$, by comparing with experimental data the aerodynamic coefficients, and also the pressure coefficient at four wing sections and the skin friction lines. In general, the best agreement with experiment is obtained on structured meshes. The standard deviation observed is about ± 1 count in lift ($\pm 3\%$) and ± 40 counts in drag ($\pm 10\%$), and even down to 5% for 4th order accurate solutions, which is reasonable if one considers the complexity of the flow at such high angle of attack. The computation of the polar confirms the trends observed at 11.22° AoA. The prediction of the lift to drag ratio is a more complex matter and its correct prediction within ± 1 was however achieved with the structured mesh of 12 million points.

3.2 Results LEX

A Leading Edge eXtension LEX are an extendable flap added between the leading edge of an aircraft's wings at the root and its fore-body, in order to improve high angle of attack manoeuvrability by modifying the vortical flow. LEX flap deflection moves the LEX vortex cores outboard and away from vertical tail plane, moves the maximum suction region toward the wing tips and further aft, and finally can help to partially re-attaches the LEX vortices to the wing. The study here corresponds to the experiments conducted at ETHZ on a scaled version of a simplified PAK-FA. In all results presented here the angle of attack is fixed at 17° and the LEX flap is either non-deflected 0° with respect to the after body flat plate or deflected at -20° as shown by the extent of deflection of the red part in the figure 3. Computations were performed with the code NSMB on 48 nodes (12 quad cores) for an average of 12 to 16 hours per computation on a 32 million structured grid of over 2000 blocks.

The flow conditions and computational mesh are identical as those measured during the wind-tunnel tests with an upstream velocity of $U_\infty = 18$ [m/s], $P_\infty = 96500$ [Pa], $T_\infty = 295$ [K] and a Reynolds number based on the mean aerodynamic chord of $Re = 5 \cdot 10^5$. The boundary conditions assume a uniform inflow velocity with imposed turbulence intensity and total pressure with constant temperature. For the outflow, a partially non-reflecting subsonic outflows condition is used. This approach [14] consists in minimising impinging perturbation while allowing smooth transients.

For the computations, the same turbulence intensity as that measured in the windtunnel was used:

$$I = u_{RMS}/U \sim 0.62\%$$

where u_{RMS} is the root-mean-square of the turbulent velocity. For all calculations the compressible RANS equations were taken and the Reynolds stresses were modelled by Menter's 2003 k- ω SST model.

Comparing total pressure survey with the experimental measurements along using cut planes normal to the aircraft axis, in figures 10, 11, show Vortex centres located by minima in the total pressure and intensity gauged by the scale of the depression. Both position and intensity of vortices were found to agree qualitatively.

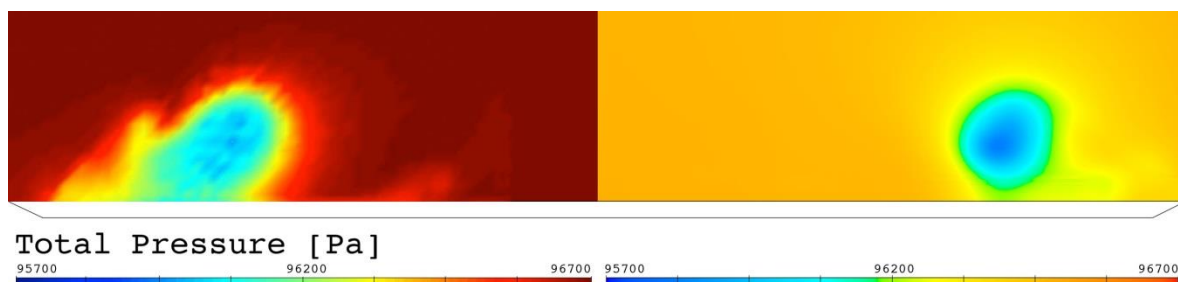


Figure 10: Total pressure experimental (left) / numerical (right) in a cut plane in the spanwise direction (Cut E from Fig. 11). Global agreement of location and intensity for vortex triggered by LEX flap deflection over a high speed wing of a generic fighter aircraft.

Three important consequences of the LEX flap deflection can be seen on the structure of the flow can be seen in Fig. 11. Firstly lowest pressure region is moved from the leading edge of LEX to the leading edge of the delta-wing and more generally the low pressure region is moved aft. Secondly, the low pressure region caused by the vortex is moved outboard. Thirdly the vertical tail-plane's (VTP) leading edge root is subject to lower pressure gradients when the LEX flap is deflected, which influences the manoeuvring capabilities at high angle of attack, The pressure survey obtained with the cut-planes, show how the LE vortex is moved outboard, and how low-pressure regions caused by the vortex are moved toward the tail of the aircraft hence avoiding strong interaction with the vertical tail plane. Also, the low pressure region is both smaller and further away from the VTP indicating a modified structure of the vortex breakdown.

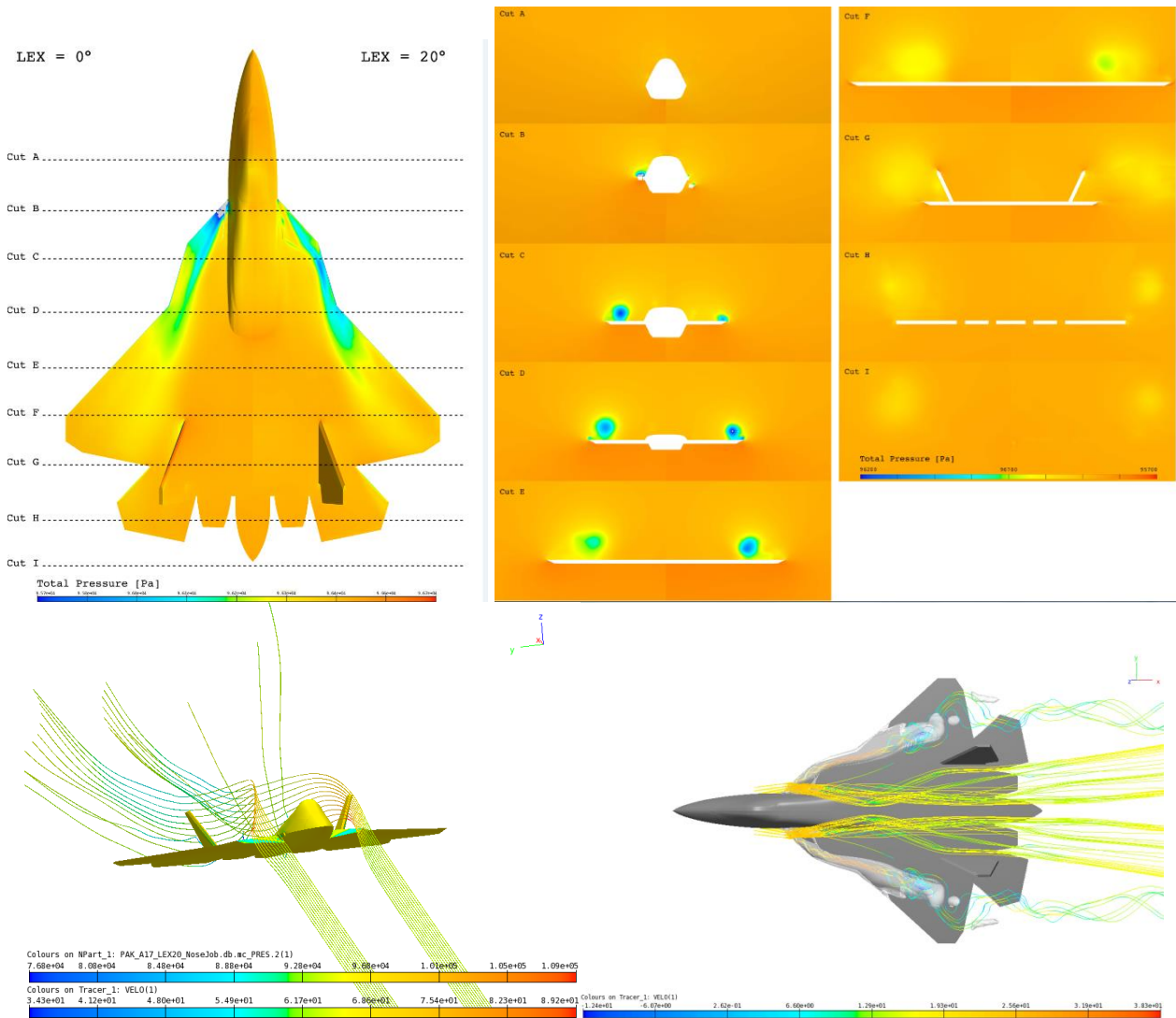


Figure 11: LEX at 0 and 20 degrees of deflection: total pressure levels on the surface(top left); vortex evolution tracked by total pressure in [Pa] down the aircraft at the different locations, (top right). Velocity streamlines for LEX 20°, (below left) showing the avoidance of the VTP with use of the LEX; and a top view with iso pressure surface of 93500 [Pa] in grey (below right)

The vortex core paths were extracted from total pressure measurements. The numerical determination of the LEX vortex core paths confirms the trends obtained from the experimental wind-tunnel measurements. At high angle of attack, the deflection of the LEX flap moves the vortex core away from the fuselage toward the wing tips, Figures 11, 13. Further similarity is shown in Figure 12 with comparisons with smoke evolution over the flap.

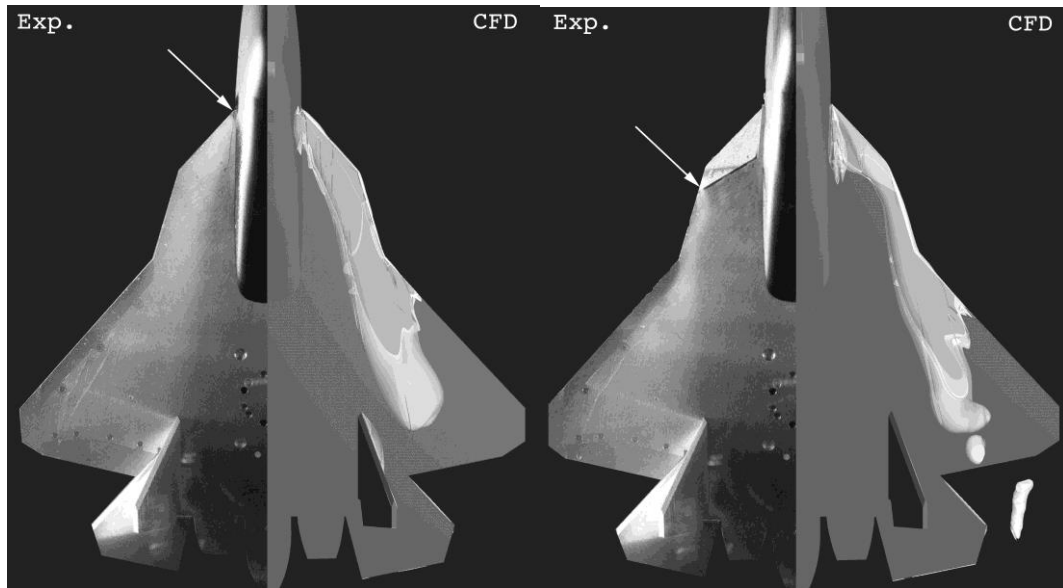


Figure 12: Smoke visualisation left and numerically obtained surface of iso-pressure at $P = 96\,300\text{[Pa]}$ right for both non-deflected LEX flap (a) and deflected flap (b). The white arrow indicates the location of the smoke source.

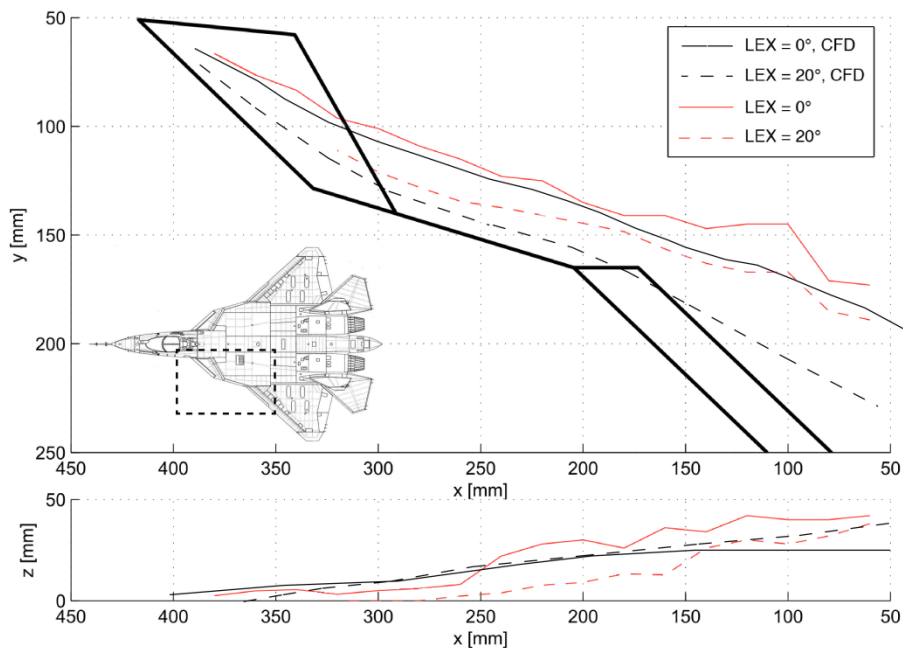


Figure 12: Comparison between experimental, in red, and numerical, in black, LEX vortex core path. Top view (above) and cut (below) with both cases of non-deflected LEX flap ($LEX = 0^\circ$) in solid lines and deflected LEX flap ($LEX = 20^\circ$) in dashed lines.

5. Conclusions and Perspectives

The role of vortices shed from or near leading edges for low-speed configurations of potentially high speed aircraft such as fast business jets, next generation stealth military aircraft and innovative new transonic transport systems, is a key design factor.

The complexity of such flows are reasonably captured by state of the art CFD solvers with high level of turbulence modelling, and high order numerical scheme accuracy. The influence of the turbulence model, the mesh size, the

convergence levels and the flow solvers from this study and similar studies show the high sensitivity to these parameters as well as an indication that RSM / SST type turbulence models predict coherent values compared to wind-tunnel experiments. However, further research must be done to provide more accurate vortex tracking CFD which tend to remain too close to the aircraft in the numerics compared to the experiments and flight. DES simulations were attempted starting from an initial RANS solution with $k-\omega$ SST, but without conclusive results. This is in part due to the stringent need of having a-priori knowledge of the flow required for specifying a judicious distance from the surface to transition from RANS to LES compatible with these complex flows. Even though 12-30 million cell meshes were used, the results were still not fully converged and even finer meshes would be required. More investigations on simpler generic geometries are required with basic experimental data to verify and validate the models.

In conclusion, CFD techniques have been evaluated and validated for the prediction of low speed flows on supersonic aircraft wing configurations featuring high-lift devices showing how the joint results from wind-tunnel experiment and CFD can be used as efficient design tools for challenging off-design regimes.

Acknowledgements

The work related in this paper was mainly supported by the FP6 projects HISAC, Environmentally Friendly High Speed Aircraft, co-ordinated by Dassault Aviation, as Task 2.5, and the FP6 European project EPISTLE1 (European Project for the Improvement of Supersonic Transport Low Speed Effects). The authors are grateful to Dassault Aviation, Airbus and DLR for their collaboration, and in particular Joel Brezillon (DLR, now Airbus). The authors acknowledge the inputs from the experimental results from ONERA and ETHZ.

References

- [1] HISAC; Environmentally Friendly High Speed Aircraft, FP6. 2005-2010.
- [2] EPISTLE, European Project for the Improvement of Supersonic Transport Low Speed Efficiency. 2002-2007.
- [3] Herrmann, U., *Low-Speed High-Lift Performance Improvements obtained and validated by the EC-project EPISTLE*, 24th International Congress of the Aeronautical Sciences, Optimage Ltd, Edinburgh, UK, 2004. and Final Technical Report of the EC-Project "EPISTLE", Tech. rep., DLR, Braunschweig, Germany, 2005.
- [4] Marc Immer, Thomas Rosgen, *Aerodynamic investigation of a variable incidence strake on a 5th generation fighter aircraft at high angle of attack*; Master Thesis, Institute of Fluid Dynamics, Swiss Institute of Technology Zurich.
- [5] BASPL++ visualisation software kit, SMR; <http://www.smr.ch>
- [6] P. Weber and L. Billeter, Bericht über die Abnahmeversuche am neuen Antrieb des Windkanals der ETH Tech. report Institute of Fluid Dynamics, ETH Zurich, 1989.
- [7] P. Leyland, S. Merazzi, J. Favre, A. Henze, H. Olivier. *ELAC: A high speed transportation system, Experiments, calculations and visualisations*. Chapter in Book: "High Speed Flows", Ed. CIMNE, 2003; ISBN: 8495999-18-8.
- [8] P. Leyland, J. B. Vos, V. Van Kemenade, A. Ytterstrom NSMB: A Modular Navier Stokes Multiblock Code for CFD. AIAA Paper 95-0568. 33rd Aerospace Meeting AIAA, Reno, January 1995.
- [9] NSMB Handbook ; J. B. Vos, P. Leyland et al. 2004.
- [10] T. B. Gatski and J.-P. Bonnet. Chapter 3 - compressible turbulent flow. In *Compressibility, Turbulence and High Speed Flow*, pages 39 -77. Elsevier, Amsterdam, 2009.
- [11] F.R. Menter Two-equations Eddy-viscosity turbulence models for engineering applications AIAA J., 32 (8) (1994), pp. 1598-1605
- [12] F.R. Menter, M. Kuntz, R. Langtry, Ten Years of Industrial Experience with the SST Turbulence Model, *Turbulence, Heat and Mass Transfer* 4, 2003.
- [13] M.Gaffuri, J. Brezillon, D. Kwak, K. Ohiraz, G. Carrier ; *Comparison of CFD solvers for low speed vortex dominated flows* ; AIAA Paper, AIAA Flight Dynamics, San Diego, July 2013.
- [14] G. Lodato, P. Domingo, and L. Vervisch. Three-dimensional boundary conditions for direct and large-eddy simulation of compressible viscous flows. *Journal of Computational Physics*, 227(10):5105-5143, 2008.